

# Cuprite Nanowires by Electrodeposition from Lyotropic Reverse Hexagonal Liquid Crystalline Phase

Limin Huang,<sup>†</sup> Huanting Wang,<sup>†</sup> Zhengbao Wang,<sup>†</sup> Anupam Mitra,<sup>†</sup>  
Dongyuan Zhao,<sup>‡</sup> and Yushan Yan<sup>\*,†</sup>

Department of Chemical and Environmental Engineering, University of California,  
Riverside, California 92521, and Department of Chemistry, Fudan University,  
Shanghai 200433, People's Republic of China

Received August 30, 2001. Revised Manuscript Received November 28, 2001

Cuprite (Cu<sub>2</sub>O) nanowires with diameter of 25–100 nm were electrodeposited from anionic surfactant sodium bis(2-ethylhexyl) sulfosuccinate reverse hexagonal liquid crystalline phase. The nanowires can be grown to up to tens of micrometers in length by simply changing the electrodeposition time. Resistivity measurements suggest improved alignment of the reverse hexagonal liquid crystalline phase under electric field during electrodeposition. The enhanced alignment of the liquid crystalline phase appears essential for the growth of nanowires with high aspect ratio. This new synthesis approach is fast and simple, and a great variety of organized assemblies are potentially available by simply adjusting the liquid crystal type and composition.

## 1. Introduction

Synthesis of nanowires of metals, semiconductors, and conductive polymers has attracted considerable interest in recent years.<sup>1–10</sup> Besides the approaches involving thermal evaporation and vapor–liquid–solid or solution–liquid–solid growth mechanisms for semiconductor nanowires,<sup>2–4</sup> the most widely used method for fabrication of nanowires is physical or chemical (e.g., electrochemical) deposition guided by an appropriate porous “hard” template such as anodized alumina,<sup>1,5</sup> track-etched polycarbonate and mica,<sup>1</sup> carbon nanotube,<sup>6</sup> zeolite/mesoporous silica,<sup>7–9</sup> and diblock copolymer matrix.<sup>10</sup> The hard template approach is effective, but some of the templates are not easy to fabricate and their removal is often required to retrieve the nanowires if separate single nanowires are desired.

Surfactant mesophases have proved to be useful and versatile “soft” templates. For example, syntheses of zeolite-like mesoporous materials using normal (oil in water) surfactant mesophases as templates are well

established.<sup>11–15</sup> Reverse (water in oil) micelles and microemulsions with spherical, cylindrical, or bicontinuous aqueous phases have been used for nanoparticle and sometimes nanowire synthesis by either coprecipitation reactions (for compounds such as BaCO<sub>3</sub>, BaSO<sub>4</sub>, BaCrO<sub>4</sub>, Ca<sub>3</sub>(PO<sub>4</sub>)<sub>2</sub>, etc.) or chemical reduction of metal ions.<sup>16–22</sup> Silver nanorods and nanowires were also obtained in the presence of organized media.<sup>23</sup> It is noted that all of the aforementioned syntheses use low surfactant concentration (e.g., 0.1 M) where micelles and microemulsions dominate.

In contrast, lyotropic liquid crystalline phases can be obtained at high surfactant concentrations. Attard and co-workers have demonstrated that normal hexagonal liquid crystalline phase can template bulk mesoporous SiO<sub>2</sub> by hydrothermal synthesis and mesoporous metal films (Pt, Sn) by electrodeposition.<sup>24,25</sup> Also, Stupp and co-workers have obtained nanostructured CdS from three different lyotropic liquid crystalline phases (hex-

\* To whom correspondence should be addressed. E-mail: yushan.yan@ucr.edu. Tel: 909-787-2068. Fax: 909-787-2425.

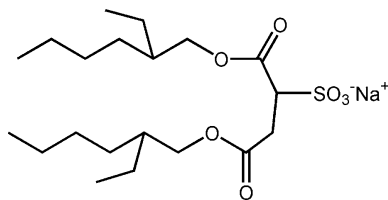
<sup>†</sup> University of California.

<sup>‡</sup> Fudan University.

(1) Martin, C. R. *Chem. Mater.* **1996**, *8*, 1739.  
(2) Pan, Z. W.; Dai, Z. R.; Wang, Z. L. *Science* **2001**, *291*, 1947.  
(3) Morales, A. M.; Lieber, C. M. *Science* **1998**, *279*, 208.  
(4) Markowitz, P. D.; Zach, M. P.; Gibbons, P. C.; Penner, R. M.; Buhro, W. E. *J. Am. Chem. Soc.* **2001**, *123*, 4502.  
(5) Zhang, Z. B.; Gekhtman, D.; Dresselhaus, M. S.; Ying, J. Y. *Chem. Mater.* **1999**, *11*, 1659.  
(6) Sloan, J.; Wright, D. M.; Woo, H. G.; Bailey, S.; Brown, G.; York, A. P. E.; Coleman, K. S.; Hutchison, J. L.; Green, M. L. H. *Chem. Commun.* **1999**, 699.  
(7) Wu, C. G.; Bein, T. *Science* **1994**, *264*, 1757.  
(8) Han, Y. J.; Kim, J. M.; Stucky, G. D. *Chem. Mater.* **2000**, *12*, 2068.  
(9) Huang, M. H.; Choudrey, A.; Yang, P. D. *Chem. Commun.* **2000**, 1063.  
(10) Thurn-Albrecht, T.; Schotter, J.; Kastle, G. A.; Emley, N.; Shibauchi, T.; Krusin-Elbaum, L.; Guarini, K.; Black, C. T.; Tuominen, M. T.; Russell, T. P. *Science* **2000**, *290*, 2126.

(11) Kresge, C. T.; Leonowicz, M. E.; Roth, W. J.; Vartuli, J. C.; Beck, J. S. *Nature* **1992**, *359*, 710.  
(12) Zhao, D.; Feng, J.; Huo, Q.; Melosh, N.; Fredrickson, G. H.; Chmelka, B. F.; Stucky, G. D. *Science* **1998**, *279*, 548.  
(13) Lu, Y. F.; Ganguli, R.; Drewien, C. A.; Anderson, M. T.; Brinker, C. J.; Gong, W. L.; Guo, Y. X.; Soyoz, H.; Dunn, B.; Huang, M. H.; Zink, J. I. *Nature* **1997**, *389*, 364.  
(14) Tanev, P. T.; Pinnavaia, T. J. *Science* **1995**, *267*, 865.  
(15) Trau, M.; Yao, N.; Kim, E.; Xia, Y.; Whitesides, G. M.; Aksay, I. A. *Nature* **1997**, *390*, 674.  
(16) Hopwood, J. D.; Mann, S. *Chem. Mater.* **1997**, *9*, 1819.  
(17) Walsh, D.; Mann, S. *Chem. Mater.* **1996**, *8*, 1944.  
(18) Tanori, J.; Pileni, M. P. *Langmuir* **1997**, *13*, 639.  
(19) Li, M.; Schnablegger, H.; Mann, S. *Nature* **2000**, *402*, 393.  
(20) Qi, L.; Ma, J.; Cheng, H.; Zhao, Z. J. *Phys. Chem. B* **1997**, *101*, 3460.  
(21) Lisiecki, I.; Pileni, M. P. *J. Am. Chem. Soc.* **1993**, *115*, 3887.  
(22) Tanori, J.; Pileni, M. P. *Adv. Mater.* **1995**, *7*, 862.  
(23) Jana, N. R.; Gearheart, L.; Murphy, C. J. *Chem. Commun.* **2001**, 617.  
(24) Attard, G. S.; Glyde, J. C.; Goltner, C. G. *Nature* **1995**, *378*, 366.  
(25) Attard, G. S.; Bartlett, P. N.; Coleman, N. R. B.; Elliott, J. M.; Owen, J. R.; Wang, J. H. *Science* **1997**, *278*, 838.

### Scheme 1. Structure of Surfactant AOT Molecule



agonal, cubic, and lamellar) by reaction between  $\text{Cd}^{2+}$  and  $\text{H}_2\text{S}$ .<sup>26</sup> Very recently, reverse hexagonal liquid crystalline phase was used as a template to synthesize ZnS nanowires ( $<2 \mu\text{m}$ ) by  $\gamma$ -ray irradiation using thiourea or  $\text{CS}_2$  as sulfur source.<sup>27</sup> The ZnS nanowires thus obtained are fairly short, probably because of poor alignment within the liquid crystalline phase.

In this study, we demonstrate that semiconductor nanowires can be fabricated by electrodeposition from lyotropic reverse hexagonal liquid crystalline phase with one-dimensional aqueous channels as space-confined microreactors. Electrodeposition is preferred because it allows easy control of growth of the nanowires by simply changing the electrodeposition time. We also show that the connectivity of the aqueous channels and alignment of the liquid crystal can be improved with the application of electric field during electrodeposition, leading to the production of nanowires with high aspect ratio.

## 2. Experimental Section

**Materials.** Anionic surfactant sodium bis(2-ethylhexyl) sulfosuccinate (AOT) (98 wt %) and oil phase *p*-xylene (99 wt %) were purchased from Aldrich Chemical Co., and  $\text{CuCl}_2 \cdot 2\text{H}_2\text{O}$  (lab grade) was from Fisher Scientific. All chemicals were used without further purification. Distilled water was passed through a Barnstead system until its resistivity reached  $17 \text{ M}\Omega \cdot \text{cm}$ .

**Preparation of Reverse Hexagonal Liquid Crystalline Phase.** Surfactant AOT is an amphiphilic molecule that has a hydrophilic anionic head and two hydrophobic chains (Scheme 1), and its phase diagram including the formation of reverse hexagonal liquid crystal is well established.<sup>28,29</sup> The liquid crystal phase is described here in the format of AOT ( $x$ )/*p*-xylene/ $\text{CuCl}_2$  ( $y$ )( $w$ ), with  $x$ ,  $y$ , and  $w$  standing for AOT concentration in *p*-xylene,  $\text{CuCl}_2$  concentration in water, and molar ratio of water to surfactant, respectively. A typical composition used in this study is AOT (1.5 M)/*p*-xylene/ $\text{CuCl}_2$  (0.1 M)( $w = 10$ – $20$ ). To prepare the liquid crystal, AOT was first dissolved in *p*-xylene. To this solution, 0.1 M  $\text{CuCl}_2$  aqueous solution was added dropwise with stirring. The mixture was stirred for 1 h to give a clear viscous liquid at  $25^\circ\text{C}$ .

**Nanowire Formation by Electrodeposition.** Electrodeposition was conducted by using a Solartron 1287 potentiostat in a two-electrode configuration, with the two electrodes narrowly spaced (0.5 mm apart) and the aforementioned surfactant liquid crystalline phases as electrolyte. A polished stainless steel plate or copper plate ( $16 \times 16 \text{ mm}$ ) was used as working electrode (cathode) to collect the nanowires. A copper thin plate ( $16 \times 16 \text{ mm}$ ) was used as the counter electrode (anode) so that only metal dissolution reaction occurred on the counter electrode to ensure that the preformed liquid crystalline phase was not disturbed by gas evolution. Static potential of  $-1.1 \text{ V}$  was applied across the two electrodes

for a certain period of time (10 min–2 h) with a current density of  $200$ – $400 \mu\text{A}/\text{cm}^2$ . After electrodeposition, the nanowire deposit on the electrode was thoroughly washed with ethanol to remove the liquid crystalline phase.

**Characterization.** Liquid crystalline phases were examined using Nikon Microphot-FXA polarizing microscope at room temperature. Scanning electron microscope (SEM) images were obtained in a Philips XL30-FEG operated at  $20 \text{ kV}$ . The samples were directly imaged in the SEM without additional metal coating. X-ray diffraction (XRD) patterns were obtained in a Siemens D-500 diffractometer using  $\text{Cu K}\alpha$  radiation. Transmission electron microscope (TEM) images and electron diffraction pattern were performed on a Philips CM300 equipped with EDX spectrometer and operated at  $300 \text{ kV}$ . The samples for TEM were prepared by scratching the wires off the electrode surface, followed by dispersion in ethanol by ultrasonication and deposition via drying onto gold grids covered with holey carbon support films.

Impedance measurement was performed on a Solartron 1260 impedance gain-phase analyzer at a frequency range of  $0.1$ – $10^5 \text{ Hz}$  and an ac amplitude between  $10$  and  $1000 \text{ mV}$ . Resistance values were taken at a low frequency of  $0.1 \text{ Hz}$  where dc-like resistance was obtained. Resistivity ( $\rho$ ) was calculated as

$$\rho = r \times s/l \quad (1)$$

where  $r$  is the resistance,  $s$  is the electrode surface area, and  $l$  is the electrode distance.

## 3. Results and Discussion

The polarized light micrographs show characteristic birefringence of a hexagonal liquid crystalline phase both before (when pure water was used) and after doping of  $\text{Cu}^{2+}$  ions (Figure 1).<sup>29</sup> This shows that the hexagonal liquid structure is retained after the addition of  $0.1 \text{ M Cu}^{2+}$  ions into the aqueous phase.

Figure 2 shows the SEM images of cuprite nanowires electrodeposited at two different deposition times. When the electrodeposition time is 1 h, a large number of nanowire bundles that are  $3$ – $5 \mu\text{m}$  in length (Figure 2a) are obtained. Higher magnification image shows that the individual nanowire bundle consists of nanowires that are approximately  $25$ – $45 \text{ nm}$  in diameter (not shown). The nanowires are usually close-packed at the end attached to the electrode and become divergent at the other end. It is noted here that the diameter of an individual nanowire is larger than that of the aqueous channels within the liquid crystalline phase.<sup>19</sup> The exact reason for the size mismatch is not clear. The size mismatch between the templated inorganic structures and the template medium has also been found in other synthesis systems such as reverse micelle, bicontinuous microemulsion, and lamellar phase.<sup>17,18,22</sup> When the electrodeposition time reaches 2 h, the nanowires are more than  $10 \mu\text{m}$  long and the diameter of the nanowire increases to about  $100 \text{ nm}$  (parts b and c of Figure 2). This shows that the diameter and length of the nanowires can be tuned by electrodeposition time. The diameter of the nanowire can also be varied by adjusting the water-to-surfactant ratio ( $w$ ). XRD pattern of the nanowires deposited on stainless steel substrate shows diffraction peaks with  $d$  spacings of  $2.47$ ,  $2.14$ ,  $1.51$ , and  $1.29 \text{ \AA}$  (Figure 3). Although the diffraction peaks are relatively weak, they match those of cuprite ( $\text{Cu}_2\text{O}$ ). The TEM image and the corresponding electron diffraction pattern of a typical cuprite nanowire obtained at deposition time of 2 h are shown in Figure 4. The nanowire

(26) Stupp, S. I.; Braun, P. V. *Science* **1997**, *277*, 1242.

(27) Jiang, X. C.; Xie, Y.; Lu, J.; Zhu, L.; He, W.; Qian, Y. *Chem. Mater.* **2001**, *13*, 1213.

(28) Ekwall, P.; Mandell, L.; Fontell, K. *Mol. Cryst. Liq. Cryst.* **1969**, *8*, 157.

(29) Rosevear, F. B.; Laboratories, M. V. *J. Am. Oil Chem. Soc.* **1954**, *31*, 628.

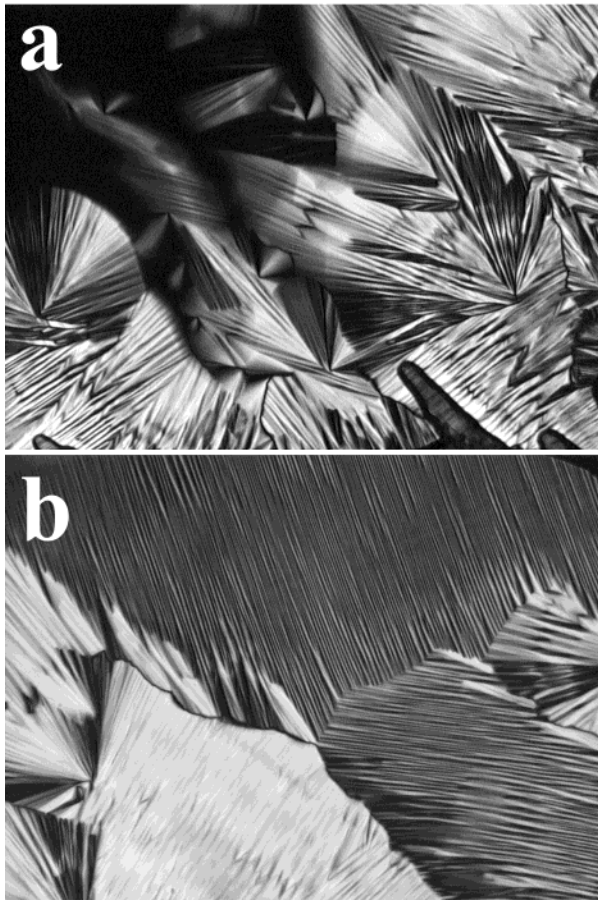


**Figure 1.** Polarized light micrographs of surfactant AOT systems ( $\times 400$ ). AOT/*p*-xylene/ $H_2O$  reverse hexagonal liquid crystal before (a) and after (b) doping of  $Cu^{2+}$  ions.

has a diameter of about 80 nm. The diffraction pattern confirms that the nanowire is crystalline but is not a single crystal.

The above electrodeposition was conducted when the two electrodes were 0.5 mm apart. When the electrode distance was increased to 1.5 mm, nanowires of poor quality were produced (not shown). If no liquid crystalline phase was used, only micrometer-sized copper crystals were produced from bulk  $CuCl_2$  aqueous solution at the deposition current density similar to that when the liquid crystalline phase was used (Figure 5).

The improved alignment of the liquid crystalline phase during deposition must be important for the formation of long nanowires. Anionic surfactant AOT in oil phase (1.5 M) has poor conductivity (resistivity =  $10^6 \Omega m$ ). This means that the conductivity of the reverse hexagonal liquid crystal comes mainly from ion movement within the aqueous channels. As a result, the resistivity of the liquid crystalline phase is expected to be a good measure of its alignment. Figure 6 shows the resistivity vs the electrode distance and AC amplitude. The resistivity remains fairly constant and high when the electrode distance is larger than 2 mm. However, it decreases dramatically with the decrease of electrode distance when the electrode distance is smaller than 1.5 mm. In addition, the resistivity also decreases with the increase of the potential across the two electrodes (ac amplitude from 10 to 1000 mV). The reduction in resistivity with the decrease of electrode distance and the increase of electrode potential seems to suggest

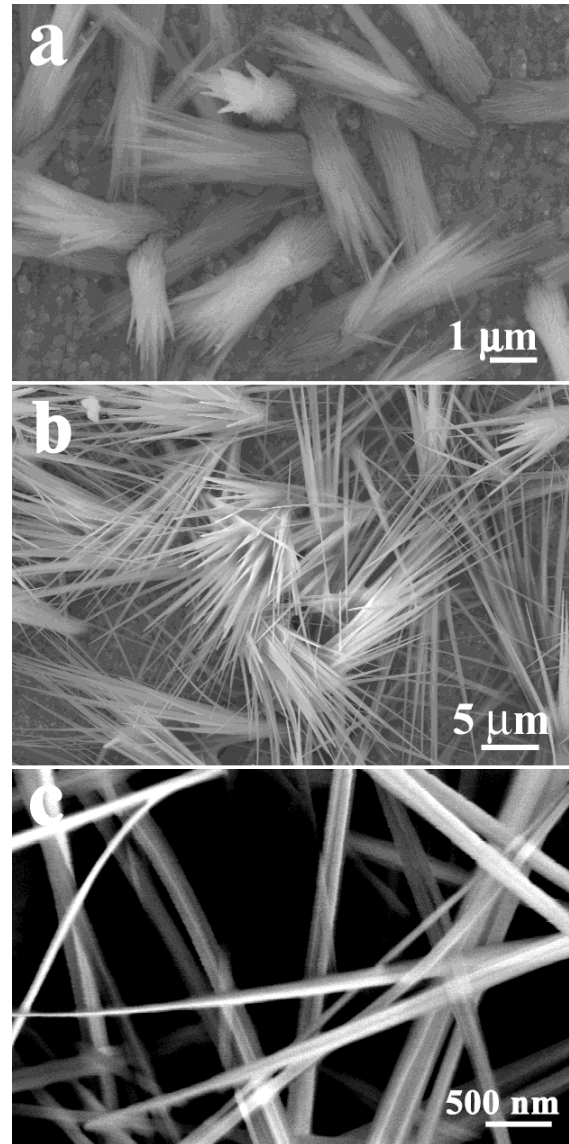


**Figure 2.** SEM images of cuprite nanowires electrodeposited from reverse hexagonal liquid crystalline phase AOT (1.5 M)/*p*-xylene/ $CuCl_2$  (0.1 M)(15) at deposition potential of  $-1.1 V$  with electrode distance of 0.5 mm for different deposition times: (a) 1 h, (b) 2 h, and (c) 2 h, at different magnifications.

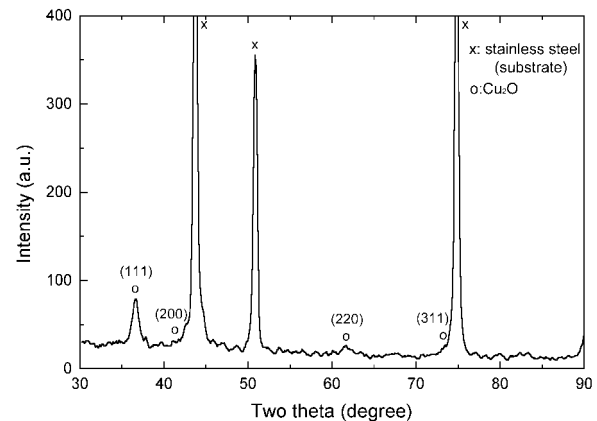


**Figure 3.** XRD pattern of cuprite nanowires electrodeposited on stainless steel electrode from reverse hexagonal liquid crystalline phase.

improved connectivity and alignment within the reverse liquid crystalline phase.

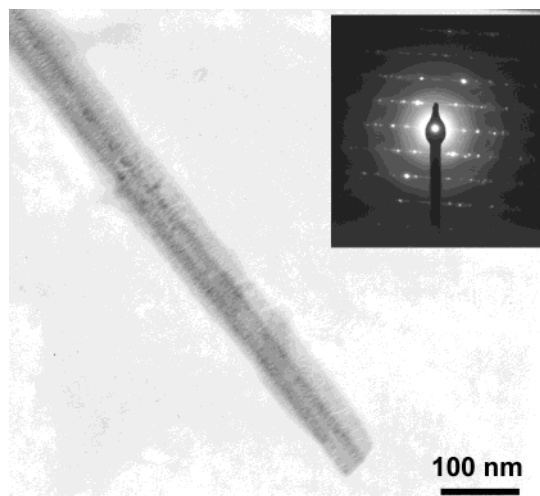


**Figure 4.** TEM image of an individual nanowire electrodeposited from reverse hexagonal liquid crystalline phase (inset, electron diffraction pattern).

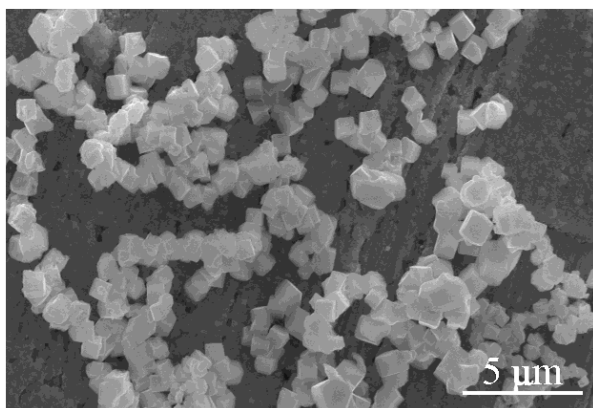


**Figure 5.** SEM images of micrometer-sized crystals electrodeposited from bulk  $\text{CuCl}_2$  aqueous solution at the similar deposition current density.

The improved alignment of the liquid crystal phase could be due to electro-osmotic flows within the one-dimensional aqueous channels.<sup>15</sup> The equation

$$v' = v/l = \rho \times i' \quad (2)$$

can be obtained from equation  $i = v/r = v/(l \times \rho/s) \rightarrow v/l = \rho(i/s)$ , where  $v'$  is the electric field gradient,  $i'$  is the current density,  $l$  is the electrode distance,  $s$  is the surface area of electrode, and  $\rho$  is the resistivity. Clearly, at constant resistivity, higher electric field gradient  $v'$  would lead to higher current density, which means higher electro-osmotic flows and better alignment within the liquid crystal. As the alignment improves, the resistivity  $\rho$  would decrease, and this decrease would enhance the current density and therefore further increase the alignment effect. To increase the electric field gradient, one option is to increase the deposition potential. However, this is not preferred because high deposition potential causes undesirable side reactions that disturb the preformed liquid crystalline phases. Thus, the decrease of distance between the two electrodes is a preferred way to increase the alignment effect. On the basis of the resistivity measurements, an improved alignment within the liquid crystal phase is proposed during the nanowire deposi-

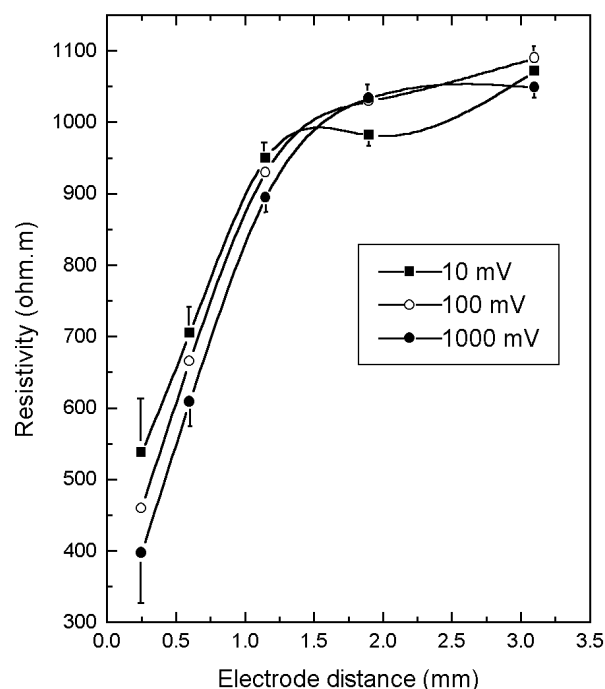


**Figure 6.** Resistivity of reverse hexagonal liquid crystalline phase AOT (1.5 M)/*p*-xylene/ $\text{CuCl}_2$  (0.1 M) (15) vs electrode distance.

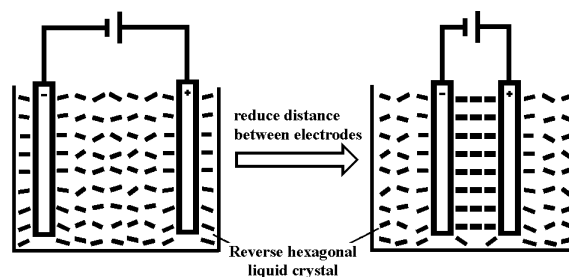


**Figure 7.** Schematic of the proposed improved alignment of the liquid crystal phase during electrodeposition.

tion (Figure 7). Although the exact templating mechanism is not completely clear, it is certain that the liquid crystalline phase has played an important role in the formation of the nanowires. Also, it is noted that the resistivity method described in the present study could become a new and effective technique for characterization of the alignment of lyotropic liquid crystalline phases.

For electrodeposition from reverse hexagonal liquid crystal containing  $\text{Cu}^{2+}$  ions, the observed product is cuprite ( $\text{Cu}_2\text{O}$ ). There are several possible routes to the formation of  $\text{Cu}_2\text{O}$ . In this study, neutral  $\text{CuCl}_2$  aqueous solution was used as the  $\text{Cu}^{2+}$  source. It is known that a recombination reaction between  $\text{Cu}^0$  and  $\text{Cu}^{2+}$  can occur to form  $\text{Cu}_2\text{O}$  in neutral medium.<sup>30,31</sup> Water molecules in surfactant mesophases have also been previously suggested as oxidants at high  $w$  (e.g.,  $w = 15$ ) in a study where the main product of reduction of  $\text{Cu}^{2+}$  by  $\text{NaBH}_4$  in a reverse micelle was  $\text{Cu}_2\text{O}$  instead of  $\text{Cu}^0$ .<sup>21</sup>  $\text{Cu}_2\text{O}$  is an important p-type semiconductor,

(30) Leger, C.; Servant, L.; Bruneel, J. L.; Argoul, F. *Physica A* **1999**, *263*, 305.

(31) Texier, F.; Servant, L.; Bruneel, J. L.; Argoul, F. *J. Electroanal. Chem.* **1998**, *446*, 189.

and its nanowires may be useful for optical and electronic applications.

#### 4. Conclusions

We have shown that  $\text{Cu}_2\text{O}$  nanowires with high aspect ratio can be readily electrodeposited from lyotropic reverse hexagonal liquid crystalline phases. Hexagonal liquid crystal phase with improved alignment plays an important role in the formation of the nanowires although the exact templating mechanism is not clear. Small electrode distance during electrodeposition ap-

pears to enhance the alignment of the liquid crystalline phase. The new approach demonstrated in this study is fast, inexpensive, reproducible, and potentially versatile for the fabrication of metal, semiconductor, and polymer nanowires.

**Acknowledgment.** We thank Professor Harry W. Green II of U. C. Riverside for access to his polarized light microscope. This work was supported in part by CE-CERT, UC-SMART, UC-TSR&TP, and UC-EI.

CM010819R